Development of a Parallel Link Arm for Object Handling by Wheeled Mobile Robot

Toyomi Fujita[1] and Hiroshi Sugawara[2]
[1]*Department of Electronics and Intelligent Systems, Tohoku Institute of Technology, 35-1 Yagiyama Kasumi-cho, Taihaku-ku, Sendai 982-8577, Japan*
[2]*Renesas Design Corp., 413 Mizuhara, Itami, 664-0005, Japan*

Keywords: Parallel Link Mechanism, Mobile Robot, Handling Task.

Abstract: This paper presents a parallel link arm for a wheeled mobile robot. A parallel mechanism is useful for a mobile robot because it has more advantages on high output power than serial link. Conventional parallel mobile manipulators have not been able to perform handling task such as picking up an object on the floor. Developed parallel link arm in this study has a hand which directs downward. It is mounted on the robot with the link for swinging so that it is able to carry an object with handling in wide area. This paper describes development of the parallel link arm and analyses its kinematics. We also consider basic motions of the arm for object handling tasks. Experimental results demonstrated the usefulness of developed parallel link arm for object handling tasks by a wheeled mobile robot.

1 INTRODUCTION

A lot of manipulation arm have been developed for a mobile robot to perform object handling tasks with movement. Although the most of them have serial link structure, there are some problems on this type: it is difficult to handle heavy object, some errors occur with respect to hand position in a motion. On the other hand, parallel link structure has some advantages such as high stiffness and higher output power at the end effector than serial link structure. Even though parallel link is not able to move in wide area, it is useful for mobile robot because the robot can move to desired position by itself so that it covers the area for manipulation to compensate the weakness of parallel link with utilizing its advantages.

Based on this consideration, some studies have presented manipulators having parallel mechanism for a mobile robot. For example, Li et al. (Li et al., 2006) presented a mobile parallel manipulator which is composed by a wheeled mobile robot with a DELTA parallel robot. Horin et al. (Horin et al., 2006) presented a parallel mechanism which was mounted on three independent carts. Yamawaki et al. (Yamawaki et al., 2004) presented a mobile parallel robot in which a parallel mechanism was mounted on tracked mobile robot. Graf and Dillmann (Graf and Dillmann, 1997) proposed a mobile robot on which a Stewart platform was mounted to compensate the unwanted accelerations. Decker et al. (Decker et al., 2001) presented a Gough-Stewart Platform mounted on a mobile robot. Shoval and Shoham (Shoval and Shoham, 2001) proposed a mobile six-DOF parallel manipulator which was used with a 3-legs robot. These types are useful for transportation of an object. However, these are not able to perform handling task such as picking up an object on the floor or ground.

In this study, we consider that the robot performs a handling task such as picking up by itself and present a novel type of a mobile parallel manipulator in which a hand directs to the ground to be suitable for object handling tasks. In addition, presented type has another link for swinging the parallel link arm in the right and left directions to get the working space large. This mechanism enables the robot to accomplish handling tasks in small space such as narrow paths without moving itself as possible.

This paper consists of the following sections: Section 2 describes the design and development of the parallel link arm. Section 3 explains analysis of kinematics of the arm. Section 4 shows basic motions for handling tasks. Section 5 employs fundamental experiments for basic motions. Finally Section 6 gives conclusions.

Fujita T. and Sugawara H..
Development of a Parallel Link Arm for Object Handling by Wheeled Mobile Robot.
DOI: 10.5220/0005116905920598
In *Proceedings of the 11th International Conference on Informatics in Control, Automation and Robotics* (ICINCO-2014), pages 592-598
ISBN: 978-989-758-040-6

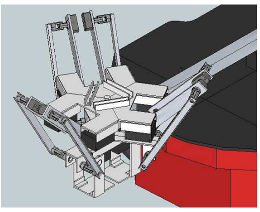

Figure 1: Concept of parallel link arm on a mobile robot

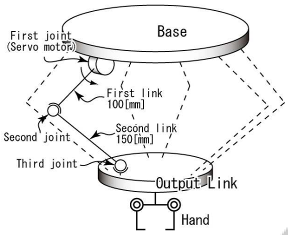

Figure 2: Mechanism of parallel link.

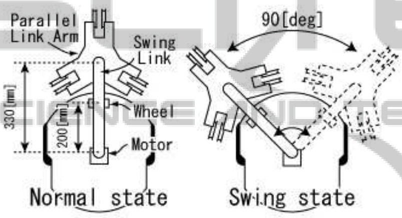

Figure 3: Concept of swing mechanism.

2 DEVELOPMENT OF PARALLEL LINK ARM

Figure 1 shows a concept of the parallel link arm which is mounted on a wheeled mobile robot. We adopted HEXA-type parallel mechanism (Pierrot et al., 1990) for the arm because this type has six-DOF and is able to move fast. A hand-unit directed to downward is also attached to the bottom of the parallel link arm so that the robot manipulate an object on the floor. In addition, we devised a swing link to change the direction of the arm. Pioneer P3-DX is used as the mobile platform.

Figure 2 shows mechanism of developed parallel link arm. The parallel mechanism has six link-units. Each link-unit consists of three joints and two links. It is attached to the base and hand-unit at both ends. The first link has 100 [mm] and the second link has 150 [mm] in length. The first joint, which is attached to the base, is active revolute joint. The second and third joints are passive and a universal joint is used for each. The hand-unit has two actuators to open and close. It is able to grasp an object which has 100 [mm] in height and 50 [mm] in wide. Kondo KRS-2552RHV is used for these eight actuators.

We have designed the base, hand-unit, and link-units using Autodesk AutoCAD. In machining them, we have generated tool-path from the CAD data using CAM software JMM-TOOL. From the tool-path, aluminum boards which have 2 or 3 [mm] in thickness have been cut by Originalmind CNC KitMill BT200 .

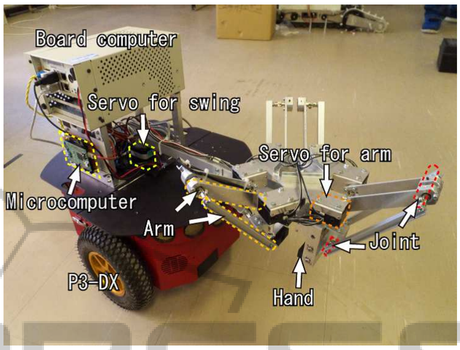

Figure 4: Robot system with developed parallel link arm.

Figure 3 shows mechanism of the swing link and concept of swinging. The parallel link arm is fixed at an end of the swing link. Another end is connected to a motor Kondo KRS-6003HV mounted at the center of top plate of P3-DX. The swing link has 330 [mm] in length so that the parallel link unit protrudes 110 [mm] ahead of the robot. A passive wheel is attached in the bottom of the swing link at 200 [mm] from the center of P3-DX to support the weight of parallel link unit. This mechanism enables the robot to change direction of the parallel link arm in 90 degrees as shown in the right panel of Fig. 3.

Figure 4 shows an overview of developed system of parallel link arm on the robot. The weight of the parallel link arm is 1.5 [kg] and that of the whole robot system is 20.5 [kg]. A board computer Interface PCI-B02PA16 and a 32-bit microcomputer Renesas RX621 are used for controlling whole robot system and parallel link arm respectively. They are mounted on the rear part of the top plate of P3-DX to be counter weight. Simple computation of moment confirmed that the maximum weight of object attached to the parallel link arm is 24.8 [kg].

3 KINEMATIC ANALYSIS

3.1 Kinematic Model of Arm

Figure 5 shows a kinematic model of a link-unit with the base, hand-unit, and swing link. We define right-hand coordinate systems for them. $\Sigma_B(x_B, y_B, z_B)$ is the base coordinate system at the center of the base. Its orthogonal unit vectors are x_B, y_B, and

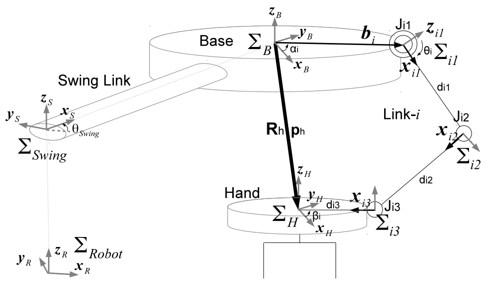

Figure 5: Kinematic model of link systems.

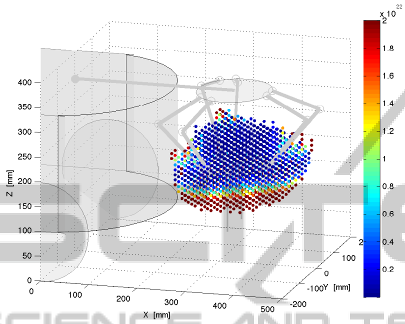

Figure 6: n_θ (norm of J_θ) to hand positions.

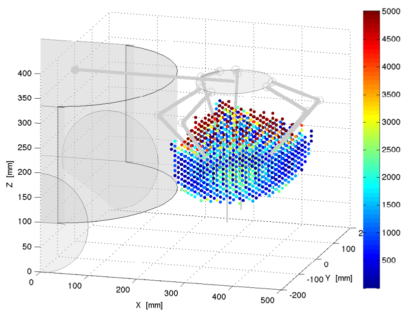

Figure 7: n_h (norm of J_h) to hand positions.

z_B. $\Sigma_H(x_H, y_H, z_H)$ is the hand coordinate system at the top center of the hand-unit, $\Sigma_{i1}(x_{i1}, y_{i1}, z_{i1})$ $(i = 1, ..., 6)$ is the coordinate systems at the active first joint for i-th link-unit. $\Sigma_{i2}(x_{i2}, y_{i2}, z_{i2})$ and $\Sigma_{i3}(x_{i3}, y_{i3}, z_{i3})$ $(i = 1, ..., 6)$ are the coordinate systems at the passive second and third joints for i-th link-unit. Let d_{i1} and d_{i2} be the lengths of the first and second links of the i-th link-unit. In addition, we define the swing coordinate system Σ_{Swing} at the rotation center of the swing link, and the robot coordinate system Σ_{Robot} at the origin of the robot.

3.2 Inverse Kinematics

Let R_{α_i} and b_i be the rotation matrix and position vector between Σ_B and Σ_{i1}. Let R_{β_i} and d_{i3} be the rotation matrix and distance between Σ_H and Σ_{i3}. These

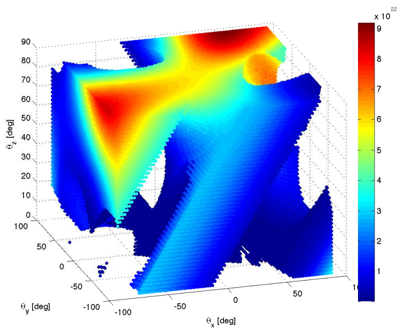

Figure 8: n_θ to hand orientations.

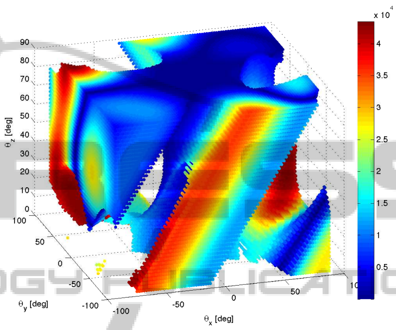

Figure 9: n_h to hand orientations.

are known because the position of the first joint and the third joint of i-th link-unit are fixed on the base and hand-unit mechanically. When translation vector p_h and rotation matrix R_h of the hand-unit to the base unit are given, the relations between links gives

$$b_i + d_{i1}x_{i1B} + d_{i2}x_{i2B} = p_h - d_{i3}x_{i3B} \tag{1}$$

where x_{i1B}, x_{i2B}, and x_{i3B} are vectors x_{i1}, x_{i2}, and x_{i3} represented in Σ_B. x_{i1B} and x_{i3B} are calculated by

$$x_{i1B} = R_{\alpha_i} R_{\theta_i} (1, 0, 0)^{\mathrm{T}}, \tag{2}$$

$$x_{i3B} = R_h R_{\beta_i} (1, 0, 0)^{\mathrm{T}} \tag{3}$$

where R_{θ_i} is the rotation matrix of the first joint of i-th link-unit; it is θ_i angle rotation around y_{i1}. From (1),(2), and (3), we can obtain θ_i by using $\|x_{i2B}\| = 1$.

3.3 Singularity

Let ω_h be the angular velocity vector of the rotation R_h. The derivative of (1) leads to

$$J_h \dot{h} = J_\theta \dot{\theta} \tag{4}$$

where $\dot{h} = (\dot{p_h}^{\mathrm{T}}, \omega_h^{\mathrm{T}})^{\mathrm{T}}$ and $\theta = (\theta_1, \cdots, \theta_6)^{\mathrm{T}}$. J_h and J_θ are 6×6 Jacobian matrices. Each row vector of J_h, $j_{h_i}^{\mathrm{T}}$ $(i = 1, \cdots, 6)$, is given by

$$j_{h_i}^{\mathrm{T}} = (d_{i2}x_{i2B}^{\mathrm{T}} \quad d_{i2}([Rx_{i3B}]_\times x_{i2B})^{\mathrm{T}}) \tag{5}$$

where $[\ ]_\times$ is a skew-symmetric matrix which represents an operation of cross product. J_θ is a diagonal matrix in which the i-th diagonal element is given as

$$J_\theta(i,i) = d_{i1}d_{i2}x_{i2B}^T \frac{\partial x_{i1B}}{\partial \theta_i}. \quad (6)$$

Gosselin and Angeles (Gosselin and Angeles, 1990) presented three kinds of singularities of parallel mechanism when

1. $\det(J_\theta) = 0$,
2. $\det(J_h) = 0$, and,
3. both of 1 and 2 occur simultaneously.

Based on this, we use the following two Euclidean norms of J_θ and J_h:

$$n_\theta = |\det J_\theta| \quad (7)$$

and

$$n_h = \sqrt{\det J_h^T J_h}. \quad (8)$$

These can be considered as manipulabilities of the parallel link arm. We have analyzed their characteristics in computer simulations.

Figure 6 and Figure 7 respectively show distributions of n_θ and n_h to hand-unit positions when the hand-unit does not rotate (R_h is the unit matrix). The position values are represented in Σ_{Robot} in the figures. The color of dots indicates the value of n_θ when the hand is at plotted position. Nothing is plotted where the parallel link arm is singularity or where it can not move the hand due to mechanical constraint. The blue area indicates the position at which it is closer to singularity. From the result of n_θ, we can see that the hand can move more stably at lower positions. On the other hand, with respect to n_h, it is close to singularity at lower hand positions.

Figure 8 and Fig. 9 show distributions of n_θ and n_h to Euler angles $(\theta_x, \theta_y, \theta_z)$ around x_B, y_B, and z_B of the hand rotation R_h when the hand-unit position is $(330, 0, 195)$ [mm] in Σ_{Robot}. In the same way, nothing is plotted at the angles by which the parallel link arm becomes singularity.

These simulation results enable us to make effective motion plannings of the robot and hand.

4 MOTIONS

4.1 Planning

From the simulation results described in Section 3, we know the workable space by the hand and swing motion without hand rotation. If the hand is in the workable space, the robot basically does not have to move. It will be better than when the robot moves itself for stable handling. Based on this consideration, a simple motion planning for a handling task was implemented. The procedure is as follows:

1. If the hand is not in whole workable space by the hand and swing motion, the robot moves to appropriate position and orientation.
2. If the hand is not in workable space by the hand only, the hand moves to appropriate position by

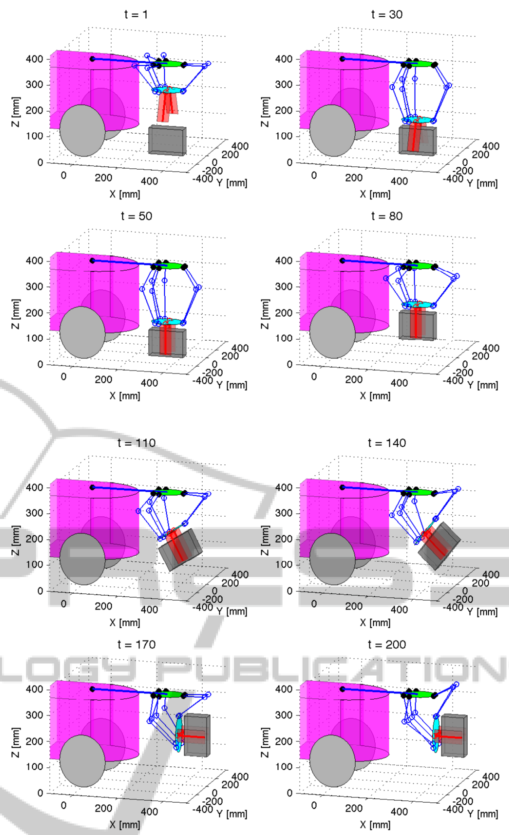

Figure 10: Forward handing motion.

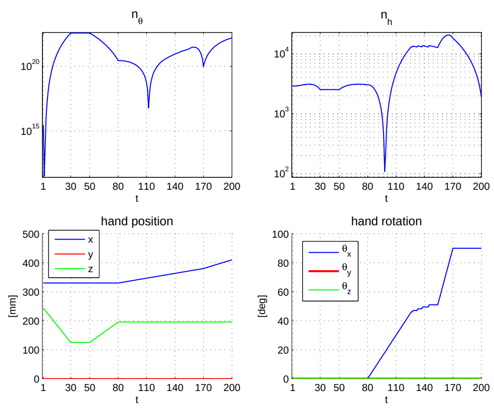

Figure 11: Simulation results in forward handing motion.

rotating swing link.

3. The hand-unit position p_{hdest} and orientation r_{hdest} at the destination are obtained according to the states of target object, where $r_h = (\theta_x, \theta_y, \theta_z)^{\mathrm{T}}$.
4. From the hand-unit position $p_h(t)$ and orientation $r_h(t)$ at current time t, desired states at the next time $p_h(t+1)$ and $r_h(t+1)$ are computed. Considering a simple straight path, these are given by

$$p_h(t+1) = p_h(t) + \frac{p_{hdest} - p_h(t)}{t_{dest}}$$

and

$$r_h(t+1) = r_h(t) + \frac{r_{hdest} - r_h(t)}{t_{dest}}$$

where t_{dest} is the time to destination from current time.

5. The norms n_θ and n_h for $p_h(t+1)$ and $r_h(t+1)$ are calculated by (7) and (8). Using thresholds v_θ and v_h, if both values meet $n_\theta \geq v_\theta$ and $n_h \geq v_h$, the hand moves to $p_h(t+1)$ and $r_h(t+1)$. Then, time is updated and goes to 4 for the next time.
6. If $n_\theta < v_\theta$ or $n_h < v_h$, the hand position or orientation is kept to be $p_h(t+1) = p_h(t)$ or $r_h(t+1) = r_h(t)$ and repeat 5. If neither case satisfies $n_\theta \geq v_\theta$ and $n_h \geq v_h$, we assume that the motion can not be achieved in current hand state, so go back to 1.

4.2 Forward Handing Motion

Figure 10 shows an example of object handling motion in which the robot picks up an object and carries it forward. The hand-unit position $p_h(t)$ and orientation $r_h(t)$ at each time step t were as described in Section 4.1. The hand starts moving down to the object at $t = 1$, starts closing at $t = 30$, and grasps the object at $t = 50$. After that, the robot picks up the object and starts rotating the hand to turn the object forward at $t = 80$. Finally, the object is oriented horizontally at $t = 170$, and moved forward slightly at $t = 200$.

Figure 11 shows transitions of norms n_θ and n_h, hand-unit position $p_h(t)$, and hand rotation $r_h(t)$ to the time step in this motion. To easily correspond to the positions in Fig. 10, the values of hand position are represented in the robot coordinate system Σ_{Robot}. We can see that θ_x, the hand rotation angle around x_B, does not change linearly around $t = 140$. It is due to a mechanical constraint caused by large angles of the third joint of the front two link-units. After the hand moves forward further, the rotation angles can change linearly.

The robot can apply this hand motion to pick up a target object and carry it to the destination with moving itself in wide area.

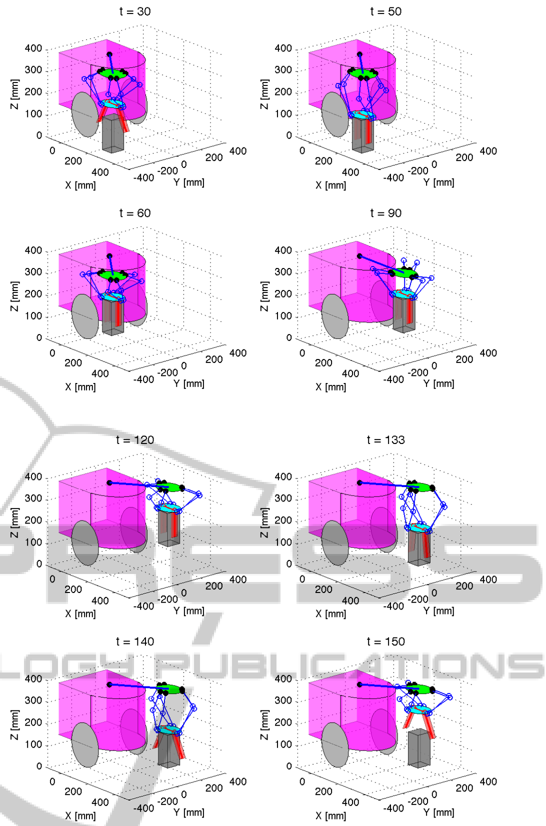

Figure 12: Pick and place motion from right to left side.

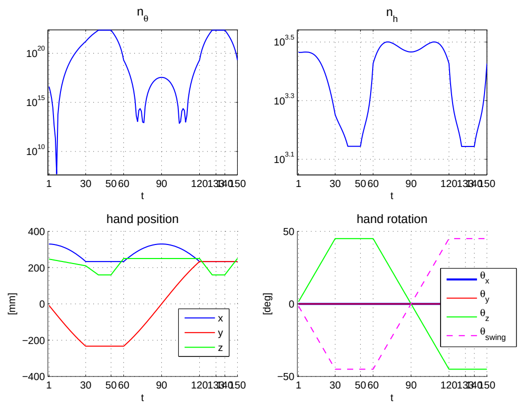

Figure 13: Simulation results in pick and place motion.

4.3 Pick and Place from Side to Side

Figure 12 shows an example of motion in which the robot picks an object at the right side, carries it to the opposite side using the swing link, and places it. After the swing link rotates to -45 degrees at $t = 30$, the hand moves down and picks up the object at $t = 60$. The swing link then starts rotating 90 degrees with keeping orientation of the object at $t = 120$, and releases the object at $t = 140$.

Figure 13 shows transitions of n_θ, n_h, $p_h(t)$, and $r_h(t)$ to the time step in this motion. Each result was obtained in the same way as previous motion. In this case, the angle of swing link θ_{swing} is changed linearly to move the hand so that the destination comes in the workable area of hand. The hand rotation angle θ_z is changed corresponding to the change of θ_{swing} to keep the orientation of the object.

5 EXPERIMENTS

5.1 Forward Handing Motion

Figure 14 shows an experiment for handing object. The robot kept grasping a B4-size notebook (panel 1 in Fig. 14), started rotating the hand after slight down (panel 2), carry the object forward (3), and handed it by opening the hand (4). It was actually difficult to rotate the hand forward so that the object orients horizontally as shown in Fig. 10 due to some mechanical constraints of the second and third joints of link-units. Nevertheless, this result indicates the ability of handing task of the robot with parallel link arm.

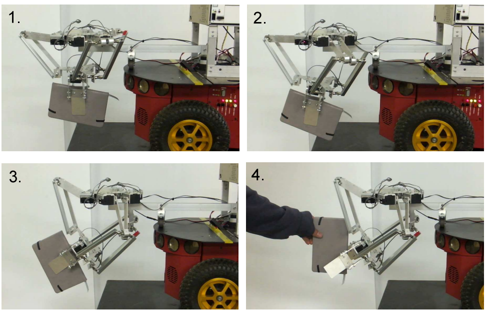

Figure 14: Handing object forward.

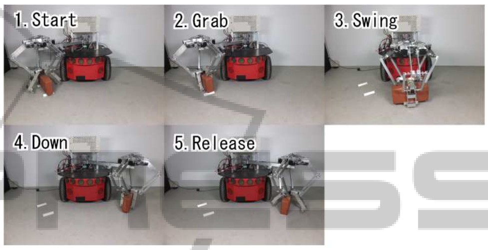

Figure 15: Picking and placing from right to left side.

5.2 Pick and Place from Side to Side

The robot carried an object from right to left with swinging motion. Figure 15 shows a sequence of the motion in this experiment. We used a 2.1 [kg] brick as the target object, which was 100 [mm] in length, 200 [mm] in width, and 52 [mm] in height. The robot moved the hand down at the right side (panel 1 in Fig. 15), started grasping the object (panel 2). After lifted it up slightly, the robot was swinging it the parallel link arm to the left side (3). The robot finally stopped swinging at the destination and touched the object to the floor (4) and released it (5). This result verified the validity of working area by utilizing the swing link.

Although it was actually difficult to move hand so as to keep its orientation as shown in Fig. 12 due to some mechanical constraints, this kind of motion shows that the robot has an ability of performing handling tasks in small space, such as an arrangement of books between book-shelves in library.

6 CONCLUSIONS

We have developed a parallel link arm to be mounted on a wheeled mobile robot. Kinematic analysis and basic motions of the parallel link arm have been presented. Simulations and experiments confirmed basic handling motions of the arm even though it had some mechanical constraints. More detailed kinematic analysis should be considered. In future, we will confirm the potential of the robot by demonstrating variety of work in wide area as well as narrow space with the advantage of parallel link by which it can handle heavier object than serial link manipulator.

REFERENCES

Decker, M., Dang, A., and Ebert-Uphoff, I. (2001). Motion planning for active acceleration compensation. In *Proceedings of IEEE ICRA 2001*, volume 2, pages 1257–1264.

Gosselin, C. and Angeles, J. (1990). Singularity analysis of closed-loop kinematic chains. *IEEE Transactions on Robotics and Automation*, 6(3):281–290.

Graf, R. and Dillmann, R. (1997). Active Acceleration Compensation Using a Stewart-Platform on a Mobile Robot 2 The mobile robots 1 Introduction. In *2nd Euromicro Workshop on Advanced Mobile Robots*, pages 59–64.

Horin, P., Djerassi, S., Shoham, M., and Horin, R. (2006). Dynamics of a six degrees-of-freedom parallel robot actuated by three two-wheel carts. *Multibody System Dynamics*, 16(2):105–121.

Li, Y., Xu, Q., and Liu, Y. (2006). Novel design and modeling of a mobile parallel manipulator. In *Proceedings of IEEE ICRA 2006*, pages 1135–1140.

Pierrot, F., Uchiyama, M., Dauchez, P., and Fournier, A.

(1990). A new design of a 6-DOF parallel robot. *Journal of Robotics and Mechatronics*, 2(4):308–315.

Shoval, S. and Shoham, M. (2001). Sensory redundant parallel mobile mechanism. In *Proceedings of IEEE ICRA 2001*, volume 3, pages 2273–2278.

Yamawaki, T., Omata, T., and Mori, O. (2004). 4r and 5r parallel mechanism mobile robots. In *Proceedings of IEEE ICRA 2004*, volume 4, pages 3684–3689.